Metal and metalloid foliar uptake by various plant species exposed to atmospheric industrial fallout: Mechanisms involved for lead

Eva Schreck, Yann Foucault, Géraldine Sarret, Sophie Sobanska, Lauric Cécillon, Maryse Castrec-Rouelle, Gaëlle Uzu, Camille Dumat

HAL Id: hal-00824725
https://hal.science/hal-00824725

Submitted on 22 May 2013

Metal and metalloid foliar uptake by various plant species exposed to atmospheric industrial fallout: Mechanisms involved for lead

E. Schreck [a,b,*], Y. Foucault [a,b,c], G. Sarret [d], S. Sobanska [e], L. Cécillon [d], M. Castrec-Rouelle [f], G. Uzu [g,h], C. Dumat [a,b,*]

[a] *Université de Toulouse; INP, UPS; EcoLab (Laboratoire Ecologie Fonctionnelle et Environnement); ENSAT, Avenue de l'Agrobiopole, 31326 Castanet Tolosan, France*
[b] *CNRS; EcoLab; 31326 Castanet Tolosan, France*
[c] *STCM, Société de Traitements Chimiques des Métaux, 30 Avenue de Fondeyre 31200 Toulouse, France*
[d] *ISTerre (UMR 5275), Université J. Fourier and CNRS, BP 53, 38041 Grenoble cedex 9, France*
[e] *LASIR (UMR CNRS 8516), Université de Lille 1, Bât. C5, 59655 Villeneuve d'Ascq cedex, France*
[f] *Université Pierre & Marie Curie (UPMC-Paris 6), Bioemco (Biogéochimie et Ecologie des Milieux Continentaux), Site Jussieu, Tour 56, 4 Place Jussieu, 75252 Paris cedex 05, France*
[g] *Laboratoire d'Aérologie (UMR 5560), OMP, UPS 14, Avenue Edouard Belin, 31400 Toulouse, France*
[h] *GET (UMR 5563), IRD, 14, Avenue Edouard Belin, 31400 Toulouse, France*

ABSTRACT

Keywords:
Foliar uptake
Particulate matter
Metals and metalloids
Internalization pathways
Microscopy
Spectroscopy

Fine and ultrafine metallic particulate matters (PMs) are emitted from metallurgic activities in peri-urban zones into the atmosphere and can be deposited in terrestrial ecosystems. The foliar transfer of metals and metalloids and their fate in plant leaves remain unclear, although this way of penetration may be a major contributor to the transfer of metals into plants. This study focused on the foliar uptake of various metals and metalloids from enriched PM (Cu, Zn, Cd, Sn, Sb, As, and especially lead (Pb)) resulting from the emissions of a battery-recycling factory. Metal and metalloid foliar uptake by various vegetable species, exhibiting different morphologies, use (food or fodder) and life-cycle (lettuce, parsley and rye-grass) were studied. The mechanisms involved in foliar metal transfer from atmospheric particulate matter fallout, using lead (Pb) as a model element was also investigated. Several complementary techniques (micro-X-ray fluorescence, scanning electron microscopy coupled with energy dispersive X-ray microanalysis and time-of-flight secondary ion mass spectrometry) were used to investigate the localization and the speciation of lead in their edible parts, i.e. leaves. The results showed lead-enriched PM on the surface of plant leaves. Biogeochemical transformations occurred on the leaf surfaces with the formation of lead secondary species ($PbCO_3$ and organic Pb). Some compounds were internalized in their primary form ($PbSO_4$) underneath an organic layer. Internalization through the cuticle or penetration through stomata openings are proposed as two major mechanisms involved in foliar uptake of particulate matter.

1. Introduction

Metal-recycling activities contribute to sustainable development. However, they also emit fine and ultrafine particulate matters (PMs) enriched with metals (Batonneau et al., 2004; Ettler et al., 2005; Nair et al., 2010; Uzu et al., 2010). In lead-recycling plants, different stages of the process (crushing, fusion, reduction and refining) are responsible for atmospheric emissions of PM enriched with various metals and metalloids: lead (Pb), arsenic (As), antimony (Sb), stain (Sn), copper (Cu), zinc (Zn) and cadmium (Cd) (Cecchi et al., 2008). PM_{10} (particulate matter with an aerodynamic diameter of 10 μm or less) is a target pollutant for the World Health Organization (WHO, 1987) and the European Commission Regulation (EC) No. 221/2002 on ambient air quality assessment (European Commission, 2002) due to its adverse effects on the environment and human health. Although $PM_{2.5}$, PM_1, and nanoparticles are minor components (in weight) of the total emitted particles, they are more critical in terms of their environmental and health impacts (Auffan et al., 2009a; Uzu et al., 2009, 2011b; Fernández Espinosa et al., 2002). In addition to its high inhalation potential (Uzu et al., 2011b), PM can deposit on terrestrial ecosystems (Donisa et al., 2000; Ma et al., 2010), leading to contamination of soils (Lin and Xing, 2007; Lee et al., 2008; Stampoulis et al., 2009; Schreck et al., 2011) and plants (Uzu et al., 2010; Hu et al., 2011). Thus, PM is a health risk for humans and grazing animals upon ingestion (Alexander et al., 2006; Polichetti et al., 2009; Perrone et al., 2010).

Unlike root transfer, which has been largely studied (Lin and Xing, 2007, 2008; Stampoulis et al., 2009; Ma et al., 2010; Yin et al., 2011; Lombi et al., 2011), little is known about metal uptake by plant leaves from the atmosphere (Tomasevic et al., 2005; Honour et al., 2009; Uzu et al., 2010). Furthermore, most of the studies on metal uptake are not recent, and have not investigated the transfer pathways involved (Little,

* Corresponding authors at: EcoLab, INP-ENSAT, Avenue de l'Agrobiopôle, BP 32607, Auzeville Tolosane, 31326 Castanet-Tolosan, France. Tel.: +33 5 34 32 39 03; fax: +33 5 34 32 39 01.

E-mail address: eva.schreck@ensat.fr (E. Schreck).

1978; Ward and Savage, 1994) or have solely focused on fallout biomonitoring (Caggiano et al., 2005; Rossini Oliva and Mingorance, 2006; Rodriguez et al., 2008; Bermudez et al., 2009; Gonzalez-Miqueo et al., 2010).

Recently, Birbaum et al. (2010) reported that smaller particles may be incorporated into leaves, whereas large agglomerates are trapped on the surface wax. Therefore, the interactions of fine particles with leaves need to be further evaluated. Tomasevic et al. (2005) found that the amount of particles deposited on leaves depended on the species due to different characteristics of the epidermis. Foliar pathways have been studied in regard to solutes and water-suspended particles (Eichert et al., 2008), organic compounds (Barber et al., 2004; Perkins et al., 2005; Moeckel et al., 2008) and gaseous elemental Hg (Millhollen et al., 2006; Stamenkovic and Gustin, 2009). To our knowledge, no recent studies have investigated uptake pathways for metals from deposited PM on leaves. Metal accumulation and pathways have been studied in lichens and mosses (Catinon et al., 2008; Godinho et al., 2009; Spagnuolo et al., 2011), but current knowledge on foliar uptake in vascular plants is still incomplete.

Recently, investigation on lead uptake by lettuce leaves, (Uzu et al. (2010)) showed that PM deposited on plant leaves may be retained by cuticular waxes and trichomes, but some of metals contained in PM can penetrate inside plant tissues. Observations performed on lettuce exposed to lead-rich fallout showed (i) fine Pb and Fe-rich particles on stomata ($PbSO_4$, PbO, $PbCO_3$ and Fe_2O_3), (ii) secondary species, such as needle crystals, enriched in lead due to transformation at the leaf surface and (iii) the presence of primary PM (with $PbSO_4$ and $PbCO_3$ as major species) under an organic layer often corresponding to necrotic zones (Uzu et al., 2010).

The main objective of the present work was to increase the understanding of the foliar uptake of metals and metalloids in the context of atmospheric PM fallout. The extent of uptake and the pathways involved may depend on the plant species and on the metal considered. In this study, we compared the accumulation of various metals (Cd, Cu, Pb, Sn and Zn) and metalloids (As and Sb) by plant species presenting contrasting morphologies and exposed to atmospheric fallouts of a lead recycling factory. The following plant species were chosen for their differences of morphology and use: lettuce and parsley (food) and ryegrass (fodder). The total concentrations of copper (Cu), zinc (Zn), cadmium (Cd), tin (Sn), antimony (Sb), arsenic (As) and lead (Pb) were measured in plants. As the major pollutant in PM emitted by a battery-recycling facility, lead was chosen to study foliar uptake mechanisms because it is concentrated enough to be detected for various microscopic and spectroscopic techniques. The localization and speciation of lead-containing PM present on and inside leaves were investigated by micro-X-ray fluorescence (μXRF), scanning electron microscopy coupled with energy dispersive X-ray microanalysis (SEM-EDX), and time-of-flight secondary ion mass spectrometry (ToF-SIMS).

These methods were chosen because they have a low spatial resolution to get elemental distribution and speciation of metals with few micrometer depth resolutions. μXRF and SEM-EDX provide an elemental distribution whereas ToF-SIMS is unique to determine both elemental distribution and speciation as a function of depth analysis. Microscopy and spectroscopy are complementary tools to determine metal distribution and speciation in leaves.

2. Materials and methods

2.1. Atmospheric fallout collection and plant exposure

Plant exposure experiments were performed in the courtyard of a secondary lead smelter that recycles car batteries. It is located in Southwest France in the peri-urban area of Toulouse (43°38′12″ N,

01°25′34″ E). The smelter emits 328 kg of total suspended particulates (TSP) each year.

In order to estimate an exposure rate of plant to metal-rich PM, the bulk metal concentrations in atmospheric fallouts were determined during the whole plant exposure period. Atmospheric fallouts were sampled in the smelter courtyard with 9.2 cm diameter high-density polyethylene (HDPE) Nalgene funnels connected to 2 L HDPE Nalgene bottles fixed on posts 2 m above ground, as described by Munksgaard and Parry (1998) and Gandois et al. (2010). The funnels and bottles were acid washed before initial use. Sample bottles filled with high purity water were used as references.

Elemental total contents of fallouts were determined by an ICP-OES IRIS Intrepid II XXDL instrument. The metal concentrations in bulk atmospheric fallouts were measured every week.

Various plant species were studied: (i) lettuce (*Lactuca sativa* L.), a leafy vegetable that has been used to test soil–plant transfer of metals (Waisberg et al., 2004; Alexander et al., 2006), (ii) parsley (*Petroselinum crispum*), an aromatic plant cultivated in kitchen gardens, presenting large foliar surfaces and a short life cycle, and (iii) ryegrass (*Lolium perenne* L.), a model plant for cattle exposure, with a longer life cycle and silicon-rich leaves. One-week-old plants were grown for 15 days in pots each containing 4 kg of uncontaminated soil in a greenhouse. Twenty-five pots of each plant species were placed for one month in the smelter courtyard under atmospheric fallout. Because this study focused on the foliar transfer of metals, a geotextile membrane was placed on the soil to protect it against atmospheric fallout and to avoid soil–plant transfer, as previously described (Uzu et al., 2010). Plants were watered from below, through pots equipped with water tank. Control plants (ten pots for each plant species) were also cultivated in the same culture devices, but placed in a greenhouse 13.2 km away from the Pb recycling facility, i.e., receiving background levels of atmospheric fallouts.

2.2. Metal concentrations in plant shoots

Five plants of each species were harvested every two weeks, and the fresh shoot and root biomasses were determined. In contrast to biomonitoring studies, tissues were washed based on human or animal ingestion. A two-step washing method with deionized water was performed for lettuce shoots (Birbaum et al., 2010; Uzu et al., 2010), whereas a single rinsing with deionized water was used for parsley as generally done before eating in a home washing process. Metal concentrations in water after washing were analyzed. Ryegrass was not washed in order to reproduce the scenario of consumption by cattle (but plants received rain washes during the culture). Plant tissues were oven-dried at 40 °C for 72 h. After mineralization of plant samples in aqua regia (mixture of 1/4 HNO_3 and 3/4 HCl) with a Digiprep instrument at 80 °C for 4 h, the Pb, Cd, Sn, Sb, As, Cu and Zn concentrations were measured by inductively coupled plasma-optical emission spectrometry ICP-OES (IRIS Intrepid II XXDL) or inductively coupled plasma-mass spectrometry ICP-MS (X Series II, Thermo Electron). Ten blanks were submitted to the same treatment (mineralization and assay) for method control. Each sample was analyzed in triplicate. The detection limits of Pb, Cd, Sn, Sb, As, Cu and Zn were 0.3, 0.2, 0.2, 0.2, 0.2, 1.3 and 2.2 μg L^{-1}, respectively, whereas the limits of quantification were about 0.4, 0.3, 0.3, 0.4, 0.3, 2 and 3 μg L^{-1}, respectively. The accuracy of measurements was checked using reference materials: Virginia tobacco leaves, CTA-VTL-2, ICHTJ and TM-26.3 certified reference material from the National Water Research Institute, Canada. The concentrations found were within 95–102% of the certified values for all measured elements.

2.3. Microscopic and spectroscopic observations

Leaf observations on a microscopic scale were performed on lettuce, parsley and ryegrass by using complementary techniques. μXRF was

used to map elemental distributions of centimeter regions of leaves with a resolution of 30 µm and a detection limit of 100 mg kg^{-1}. The morphology and elemental composition of PM deposits were determined at a higher resolution by SEM-EDX, which has a low sensitivity (about 1000 mg kg^{-1}) but a better lateral resolution than µXRF. Finally, ToF-SIMS was used to map Pb-containing molecular fragments on localized metal-enriched areas of lettuce leaves to measure the penetration of particles throughout the leaves.

2.3.1. Micro-X-ray fluorescence (µXRF)

Elemental distributions in leaves were observed by µXRF as described by Uzu et al. (2010). µXRF measurements were performed on freeze-dried leaves. An EDAX Eagle III XRF spectrometer equipped with an Rh anode and a polycapillary, which focuses the X-ray beam down to 30 µm full width at half maximum (FWHM), was used. An EDX detector with a resolution of 140 eV was used to measure the X-ray fluorescence. The spectrometer was operated at 20 kV and 300–450 µA. Centimeter sized X-ray maps were collected over 256 by 200 pixels with steps of 30–50 µm. The counting time was 600–2000 ms per pixel. Additionally, a set of 27 point µXRF spectra was acquired on metal-rich regions on ryegrass. The spectral dataset was used to statistically determine elemental associations in leaves (see Section 2.4).

2.3.2. Scanning electronic microscopy coupled with EDX (SEM-EDX)

Element distributions and leaf-specific morphologies were studied using an SEM-EDX instrument (Jeol JSM 6400 SEM) equipped with a Bruker SPD analyzer operating at 20 kV. Portions of leaves were dried, fixed on a carbon substrate and covered with carbon before analysis. Environmental SEM-EDX measurements using a Quanta 200 FEI instrument equipped with a Quantax EDX detector were also carried out to control the morphology and elemental composition of the analyzed area before ToF-SIMS measurements. Leaves were dried and fixed on a carbon substrate without any further preparation before analysis. The apparatus was operated in low-vacuum mode (~133 Pa) at 25 kV.

2.3.3. Time-of-flight secondary ion mass spectrometry and imaging (ToF-SIMS) for depth profiling

Surface analysis was performed on lettuce leaves using ToF-SIMS in the necrotic zones enriched with metals. Dried leaf tissue was mounted directly into the instrument sample holder without any further preparation and then examined at room temperature. Regions of interest which were identified using SEM-EDX were systematically investigated in Tof-SIMS experiments. Positive and negative spectra and ion images were obtained on a Tof-SIMS 5 instrument (IONTOF, Münster, Germany) equipped with 25 Kev Bi$^+$ or Bi^{3+} primary ion sources and a reflectron mass analyzer. A pulsed low-energy electron-flood gun (0.6 nA DC) was used for charge compensation. Static SIMS spectra were recorded over an area of 500×500 µm using the Bi$^+$ or Bi^{3+} sources. Under the employed experimental conditions, the mass resolution (m/Δm) ranged from 2000 to 8000 (fwhm) at m/z 500 depending on the sample. Positive and negative images were recorded over an area of 500×500 µm with 256×256 pixels using the Bi^{3+} source operating at 25 KeV with a spot size of about 1 µm. The Bi^{3+} source provided better ionic yield for organic species compared to Bi$^+$. Raw data streams were acquired in which the complete spectrum was recorded at each pixel of the image, allowing for reconstruction of spectra from chosen regions (retrospective microanalysis) or reconstruction of chemically specific images based on the intensity of chosen peaks from the average spectrum (retrospective chemical imaging). The data were acquired in static mode. Depth profiles were also recorded. Two ion beams were operated in dual beam mode. The first beam was used to sputter a crater, while the second beam progressively analyzing the bottom of the crater. An area of 890×890 µm was sputtered using Cs$^+$ or O$_2^-$ beam sources both operating at 0.5 kV. Analyses were

performed over an area of 500×500 µm with the Bi^{3+} source. The sputtering time was fixed to 1500 s for depth analyses under 100 nm. The depth thickness was calculated using the sputtering yield (comprising between 1 and 4) and atom density of the analyzed component (here 3×10^{22} atom cm^{-3}). For all measurements, accurate mass calibration of positive and negative spectra was carried out using low-mass single component default peaks.

2.4. Statistical analysis

Metal concentrations in plants were subjected to analysis of variance (ANOVA), using the software Statistica, Edition '98 (StatSoft Inc., Tulsa, OK). Significant differences (p-value < 0.05) were measured by the LSD Fisher test.

The point µXRF spectra recorded on ryegrass was subjected to principal component analysis (PCA) to investigate elemental associations in leaves (see Supporting information for more details). Differences between µXRF spectra and relationships among elemental contents were assessed by screening the ordination of the spectra in a factorial map based on the scores of the first two principal components. The corresponding loadings (the weights for each variable when calculating the first two principal components) were also examined on a two-dimensional canonical graph (a correlation circle in which the direction and length of arrows allow for evaluating the correlation between variables and the relationships between variables and principal components). Then, tentative grouping of spectra into three families was performed to highlight different types of elemental associations. A Monte Carlo test was performed with 1000 permutations to confirm the significance of this grouping (see e.g., Pascault et al., 2010). PCA of µXRF spectra was conducted using R software version 2.12 (R Development Core Team, 2010) with the ade4 package (Chessel et al., 2004).

3. Results and discussion

3.1. Influence of metals and plant species on foliar uptake

The rate of bulk atmospheric deposition was estimated to be about 325.2 ± 12.8 mg.cm^{-2} week^{-1}, with 139.4 ± 7.8 mg.cm^{-2} week^{-1} of lead. All results concerning metal and metalloid concentrations in atmospheric fallouts recorded during the entire exposure period are given in Table 1 (concentrations ± standard deviation).

As in atmospheric fallouts, lead was found to be the most concentrated metal in plant shoots. After four weeks of exposure, its concentration reached approximately 125, 300 and 700 mg Pb.kg^{-1} of dry weight for lettuce, parsley and ryegrass shoots, respectively. Antimony, tin, arsenic and cadmium concentrations were significantly (ANOVA, p < 0.05) higher in exposed plants than in the controls. The copper and zinc concentrations in shoots were slightly increased relative to the controls in parsley and ryegrass leaves only.

After only two weeks of exposure to atmospheric fallouts, the metal contents in plant shoots were relatively high (Table 1): the Pb content reached about 100 mg.kg^{-1} DW in lettuce and parsley and 300 mg.kg^{-1} DW in ryegrass. These values are largely higher than the threshold set by the European Commission Regulation (EC) No. 221/2002 for leafy vegetables and fresh herbs, (0.3 mg.kg^{-1} FW, which is about 6 mg.kg^{-1} DW). Similarly, Cd concentrations of 1.7, 0.8 and 1.6 mg.kg^{-1} DW were found for lettuce, parsley and ryegrass, respectively, compared to limit values of 0.2 mg.kg^{-1} of fresh weight, which is about 4 mg.kg^{-1} DW (Kabelitz and Sievers, 2004). These values are one to two orders of magnitude higher than those obtained in soil–root metal transfer with the same PM at a concentration of 1650 mg.kg^{-1} of PM in soils (15.2 and 1.6 mg.kg^{-1} DW in plant shoots, for Pb and Cd, respectively) (Uzu et al., 2009). These data suggest that the foliar pathway for metal uptake may be predominantly the soil–root pathway in urban and industrial environments. In the present study,

Table 1
Metal and metalloid concentrations in plant shoots (mg kg^{-1} of dry weight) and in atmospheric fallouts (mg cm^{-2}). Results are expressed as the mean of five replicates $\pm$ SD. Zn and Pb concentrations were determined by ICP-OES whereas other concentrations were determined by ICP-MS.

Metal and metalloid concentrations in plants (mg.kg^{-1} of dry weight $\pm$ SD)								
		Cu	Zn[a]	Cd	Sn	Sb	As	Pb[a]
Lettuce	Controls	6.1 ± 1.1	29.5 ± 3.9	0.4 ± 0.1	0.2 ± 0.1	0.1 ± 0.0	0.6 ± 0.1	2.1 ± 0.2
	After 2 weeks	6.3 ± 0.3	31.6 ± 2.5	1.7 ± 0.2	0.9 ± 0.1	0.8 ± 0.1	0.6 ± 0.0	107.4 ± 8.6
	After 4 weeks	6.8 ± 0.6	29.1 ± 1.5	1.7 ± 0.1	1.3 ± 0.1	1.4 ± 0.2	1.1 ± 0.1	122.0 ± 5.5
Parsley	Controls	2.3 ± 0.1	19.6 ± 0.8	0.5 ± 0.1	1.0 ± 0.1	0.2 ± 0.1	0.2 ± 0.1	0.7 ± 0.1
	After 2 weeks	2.4 ± 0.1	23.4 ± 2.1	0.6 ± 0.1	4.9 ± 0.3	1.0 ± 0.0	0.3 ± 0.0	96.0 ± 9.7
	After 4 weeks	4.4 ± 1.7	25.4 ± 1.9	0.8 ± 0.1	7.9 ± 1.9	1.8 ± 0.2	0.4 ± 0.0	298.7 ± 33.1
Ryegrass	Controls	5.5 ± 0.1	26.5 ± 2.9	0.8 ± 0.2	2.0 ± 0.3	0.6 ± 0.1	0.2 ± 0.0	4.7 ± 0.2
	After 2 weeks	5.9 ± 0.1	26.5 ± 2.9	0.8 ± 0.1	13.3 ± 1.4	1.0 ± 0.1	0.5 ± 0.0	320.2 ± 11.1
	After 4 weeks	7.0 ± 0.1	32.1 ± 1.2	1.6 ± 0.1	16.4 ± 0.7	4.5 ± 0.1	0.8 ± 0.0	700.1 ± 27.5
Metal and metalloid concentrations in atmospheric fallouts (mg.cm^{-2} $\pm$ SD)								
	Cu	Zn[a]	Cd	Sn	Sb	As	Pb[a]	
For 4 weeks	1.7 ± 0.2	$6,9 \pm 0.8$	0.9 ± 0.1	2.6 ± 0.5	1.9 ± 0.3	0.2 ± 0.0	456.2 ± 6.4	

[a] Determined by ICP-OES whereas the others were determined by ICP-MS.

some PM are ultrafine, i.e., sub-micronic and nanoparticles as observed by SEM-EDX (not shown) inducing a high reactivity with a large specific surface of PM (Auffan et al., 2009b). Foliar uptake is likely favored by these PM morphologies and the use of young plants (three-week old).

Indeed, according to Guderian et al. (1985), plants accumulate more atmospheric pollutants during the first stages of their development.

Most of the metal concentrations, particularly lead, were higher in ryegrass than in lettuce and parsley (Table 1). The washing process
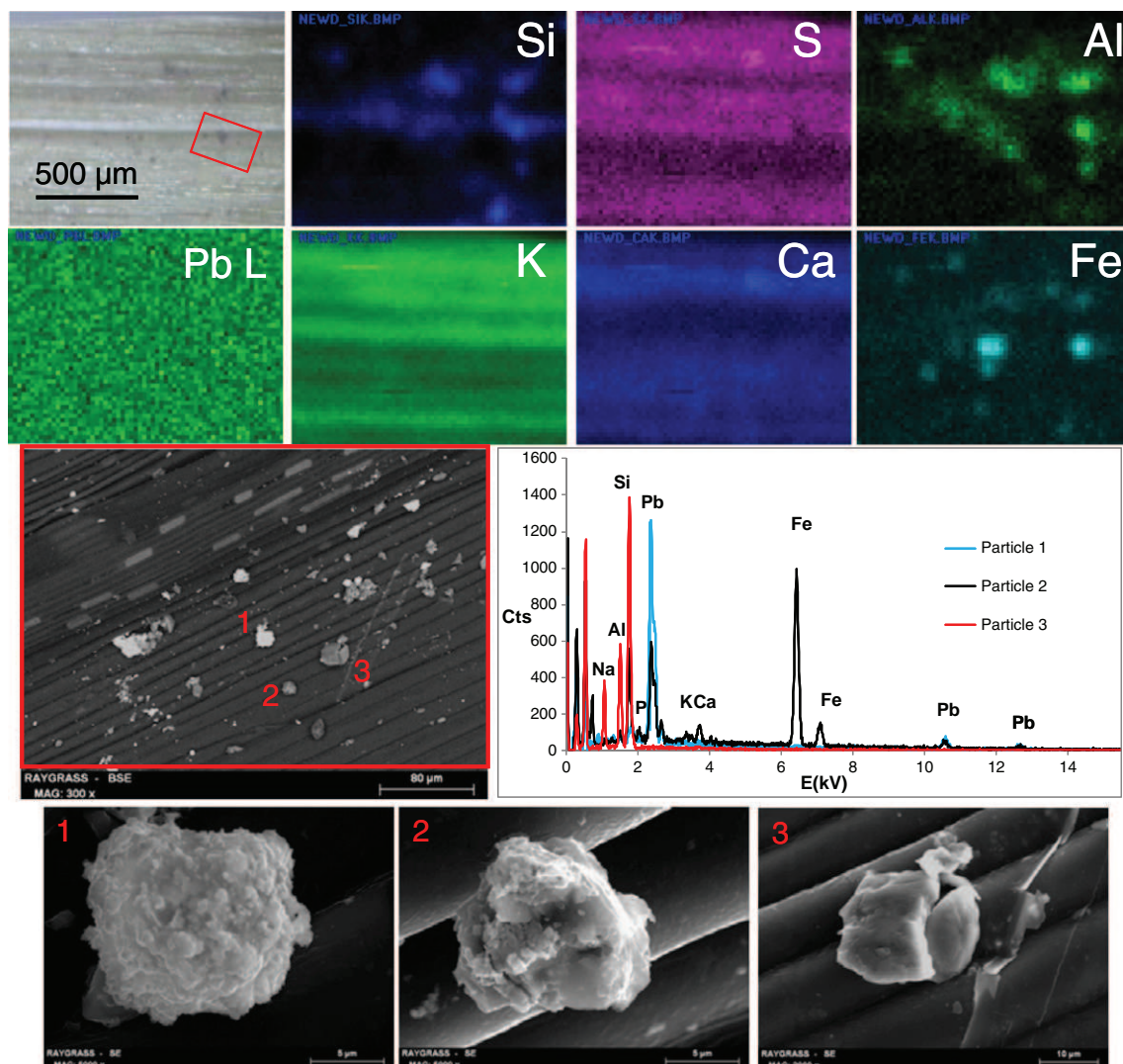

Fig. 1. µXRF elemental maps obtained for a portion of rye-grass leaf, and SEM-EDX analyses in the red triangle region. The EDX spectra for the particles noted 1, 2 and 3 are shown. Particle 1 is an aggregate of sub-micrometer-sized particles of metallic Pb, particle 2 is rich in Fe and Pb, and particle 3 is probably an alumino silicate.

contributed to a loss factor of about 25% for lead, suggesting that a part of the PM was removed by washing. However, after four weeks, the amount of lead still remained 3 and 7 times higher in ryegrass than in parsley or lettuce, respectively (Table 1). The washing process cannot fully explain the metal retention in ryegrass. The differences in plant morphology and physiology may be responsible for the differences in metal contents observed in our plant samples. Barber et al. (2004) reported that many factors may affect the air–vegetation transfer including plant characteristics such as functional type, leaf surface area, cuticular structure and leaf longevity. Little (1978) and Madany et al. (1990) showed that rough and hairy leaves accumulate significantly more lead (up to 10-fold) than smooth leaves. Rao and Dubey (1992) reported that morphological factors such as stomatal index and trichome density and length affect the efficiency of dust collection by plants. These hypotheses of surface structure were confirmed by scanning electron microscopy (SEM) images of plant surfaces (Fig. S1). Although the leaf surface of ryegrass is hairless, the plant morphology with many long leaves and silicon-enriched parallel structures (Fig. S1 — A1) with an upper surface evenly ribbed favors the interception of fine atmospheric PM as observed in Fig. S1 — A4. Birbaum et al. (2010) showed that adsorption on the leaves is reasonable, as the finest particles prefer to locate in the interphases of systems. Ryegrass was classified as a good bioindicator for heavy metal atmospheric pollution (Garrec and Van Haluwyn, 2002; NF X43-901, 2008). According to Richmond and Sussman (2003) or Da Cunha and Do Nascimento (2009), silicon largely present in ryegrass leaves (as shown in Fig. S1 — A1) might favor its metal tolerance. Although parsley is hairless as well, it forms a rosette of tri-pinnate finely cut leaves. Thus, parsley can serve as a good filter for atmospheric PM with its rough leaves to trap particles (Fig. S1 — B). Moreover this plant species exhibits a distinct specific leaf surface area due to the dissected shape of its leaves, as shown by the SEM images in Fig. S1 — B. As reported by Schreiber and Schönherr (1992), specific leaf surface areas could explain differences in rates of uptake between plant species. Lettuce leaves exhibit wide and smooth areas with small-sized granular structures (Grzegorzewski et al., 2010). They have a lower specific surface compared to the other plants studied but still present a large surface exposed to atmospheric fallout (Fig. S1 — C). Their leaves are sensitive and highly damaged by environmental stresses; necrotic zones were largely observed in the plant surface (as shown by the Fig. S1 — C7). Ward and Savage (1994) measured the Pb content in various plants exposed to road traffic emissions. Although washing protocols differed from the present study, they observed the same order for lead contents in plants: grass > aromatic plants > leaf–vegetables > cereals > fruits.

3.2. Mechanisms potentially involved on a microscopic scale μXRF and SEM-EDX observations of plant leaves

In ryegrass leaves, particles of several micrometers in diameter, most often consisting of aggregates of sub-micrometer sized particles, were observed on leaf surfaces by SEM-EDX (Fig. 1). Metallic Pb- and
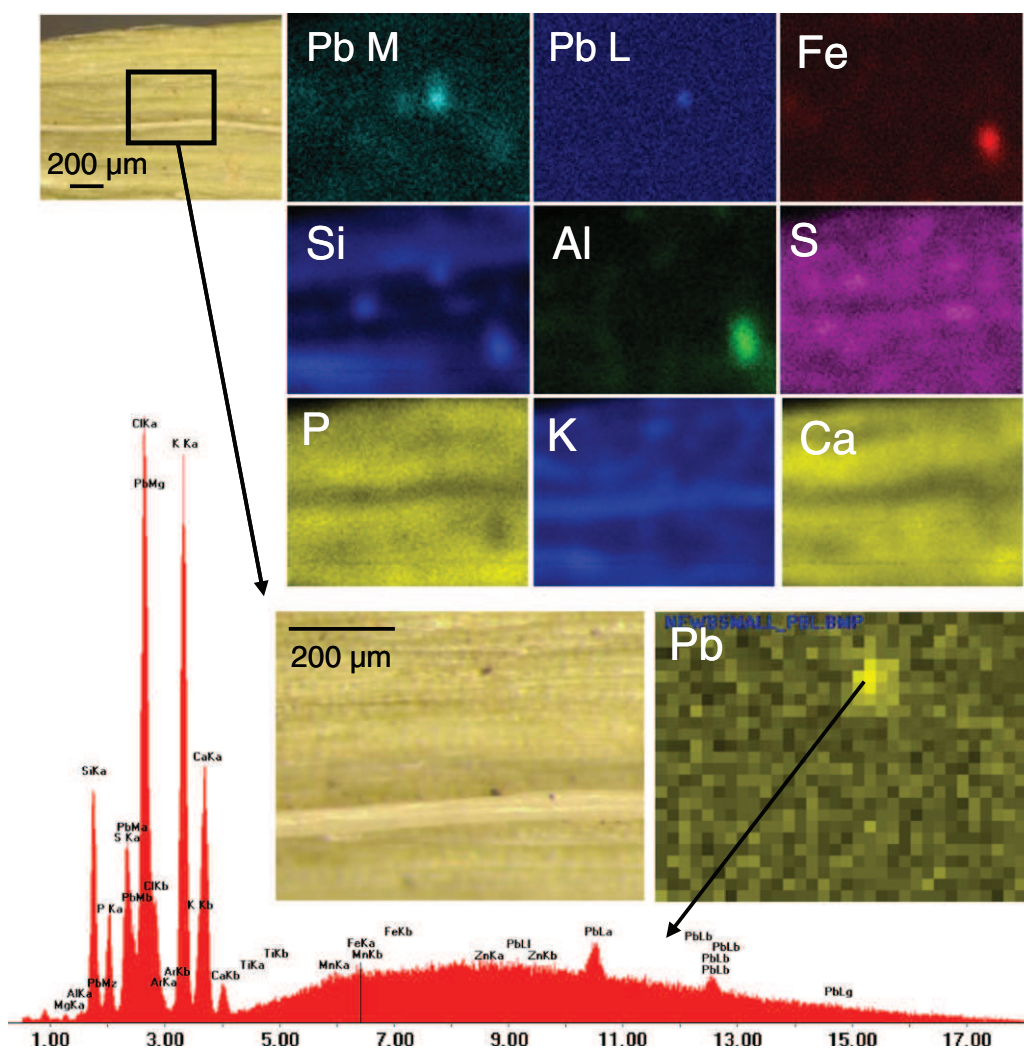

Fig. 2. μXRF elemental maps obtained for a portion of rye-grass leaf, and μXRF spectrum of the Pb-rich spot.
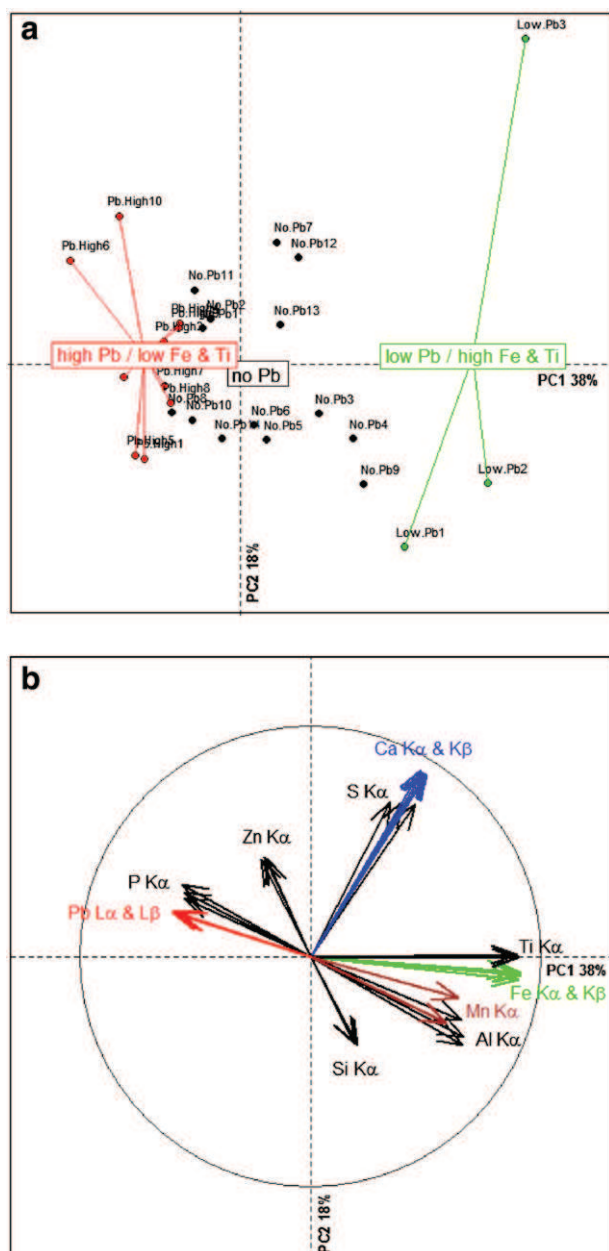
Fig. 3. Results of the principal component analysis of the set of μXRF spectra. a: Representation of the spectra in the PC1–PC2 plane. b: Correlation circle representing the 39 variables used for the PCA in the PC1–PC2 plane.

Pb–Fe-rich grains were identified as well as aluminosilicate particles attributed to industrial and soil-derived particles, respectively. Some Pb-rich regions were larger than the particles observed on the leaf surface (Fig. 2). Because of the relatively weak resolution (about 30 μm), μXRF spectra most likely integrate the signal of several particles and the leaf tissue. Considering the size of the particles, it may be difficult to characterize individual particles by this technique. Therefore, a statistical analysis was tested on a set of 27 μXRF spectra recorded on ryegrass. All 27 point spectra (Fig. S2) contained peaks assigned to P, K, S, Si (Kα emission line), Ca and Cl (Kα and Kβ emission lines). Some of them also contained peaks corresponding to Al, Mn, Ti, Zn (Kα emission line), Fe (Kα and Kβ emission lines) and Pb (Lα and Lβ emission lines). Results of the principal component analysis are shown in Fig. 3. The first two principal components accounted for 56% of the total variance (Fig. 3a). The main differences in elemental contents were observed along the first axis of the PCA (PC1 = 38% of total variance), which was mainly associated with Fe, Ti, Al, Mn, Pb and P, in decreasing order of

importance, as revealed by examination of the PCA loadings in the correlation circle (Fig. 3b). The second axis of the PCA (PC2 = 18% of total variance) was mainly associated with Ca, S, Zn, Si and Al. Detailed examination of the PCA correlation circle provided additional information on elemental associations in plant leaves (Fig. 3b and details in Supporting information). Fe and Ti were highly and positively correlated but were negatively correlated with Pb (Fig. 3b). These elements probably come from mineral dust, due to soil re-suspension in the atmosphere (Dall'Osto et al., 2010). However, this negative correlation did not signify a total separation of Fe–Ti and Pb in plant leaves, as shown by the ordination of the spectra in the PC1–PC2 factorial map (Fig. 3a). High and positive correlations between Al and Si were also observed on the PCA correlation circle (Fig. 3b). The latter suggests the presence of alumino silicate particles on plant leaves, which was confirmed by SEM-EDX (Fig. S1). Three populations of spectra were significantly discriminated by PC1 (Monte-Carlo test, p value<0.001): (i) spectra with high Pb and low Fe–Ti levels, (ii) spectra with no Pb and intermediate Fe–Ti levels, and (iii) spectra with low Pb and high Fe–Ti levels (Fig. 3a). The high Pb and low Fe–Ti spots likely correspond to primary Pb compounds emitted by the smelter. Previous characterization of the process particles allowed for identification of Pb^0, PbS, $PbSO_4$, $PbO.PbSO_4$ as major lead species (Uzu et al., 2009). Because this group contained only three spectra, other types of minor Pb-secondary species may have been missed. Analysis of a larger set of spectra would be required to identify them. The no Pb groups may correspond to mineral dust of soil origin.

Parsley leaves were observed by μXRF and SEM-EDX. Aggregates of particles<1 μm were observed on the surface. As previously suggested by the SEM observations of the leaf morphology (Fig. S1), the applied washing processes appeared to be insufficient for removing all the deposited PMs. Some of particles contained metallic Pb (Fig. 4). Other Pb-containing particles were enriched in Fe and Mn, Ca and K as well, which may correspond to ultrafine particle aggregation. The set of μXRF spectra was too small to perform PCA analyses and highlighting element correlations. Some particles (<2 μm) were located near and at the edge of the stomatal openings (Fig. 4). Similarly, SEM-EDX measurements were carried out on lettuce shoots, fine particles were observed inside stomatal openings (Fig. S1) which confirmed our previous observations (Uzu et al., 2010). Kozlov et al. (2000) studied the transfer of Cu and Ni-rich particles in birch, and suggested that particles may penetrate inside leaves through stomata. Fernandez and Eichert (2009) proposed that particles could penetrate inside the leaf tissue through pores present on the leaf cuticle and inside stomata. The diameter of cuticular pores was estimated to about 2 nm by Eichert and Goldbach (2008) and between 0.45 and 1.18 nm by Schönherr (2006). Stomatal pores were estimated to be slightly larger, a few tens of nm (Eichert et al., 2008). According to Uzu et al. (2011a), the finest PM emitted by the recycling industry is larger than 2 nm, so they could not enter by cuticular pores but could penetrate through stomatal openings.

Inorganic elements may also penetrate inside leaves after PM dissolution depending on humidity, temperature and PM characteristics (Schönherr and Luber, 2001). Moreover, as suggested by Gandois et al. (2010) and Eichert and Goldbach (2008), metal concentrations and speciation in leaves could be modified by interactions on the phyllosphere between PM and microbes. Needle crystallites enriched in Pb, not observed in the fallout PM, were observed on the parsley surface (Fig. 5-a). This was also observed in our previous work on lettuce (Uzu et al., 2010). They likely correspond to Pb-containing secondary compounds that could be due to transformations occurring after contact with the leaf. The various hypotheses are as follows: (i) changes of temperature and humidity transform PM at the leaf surface (ii) changes due to phyllosphere activity (Lindow and Brandl, 2003; Uzu et al., 2010). The second hypothesis was supported by absence of needle particles in aged PMs collected in the atmosphere (results not shown). Molecular characterization of these crystals by micro-analytical techniques is in progress. Observations with higher magnification showed
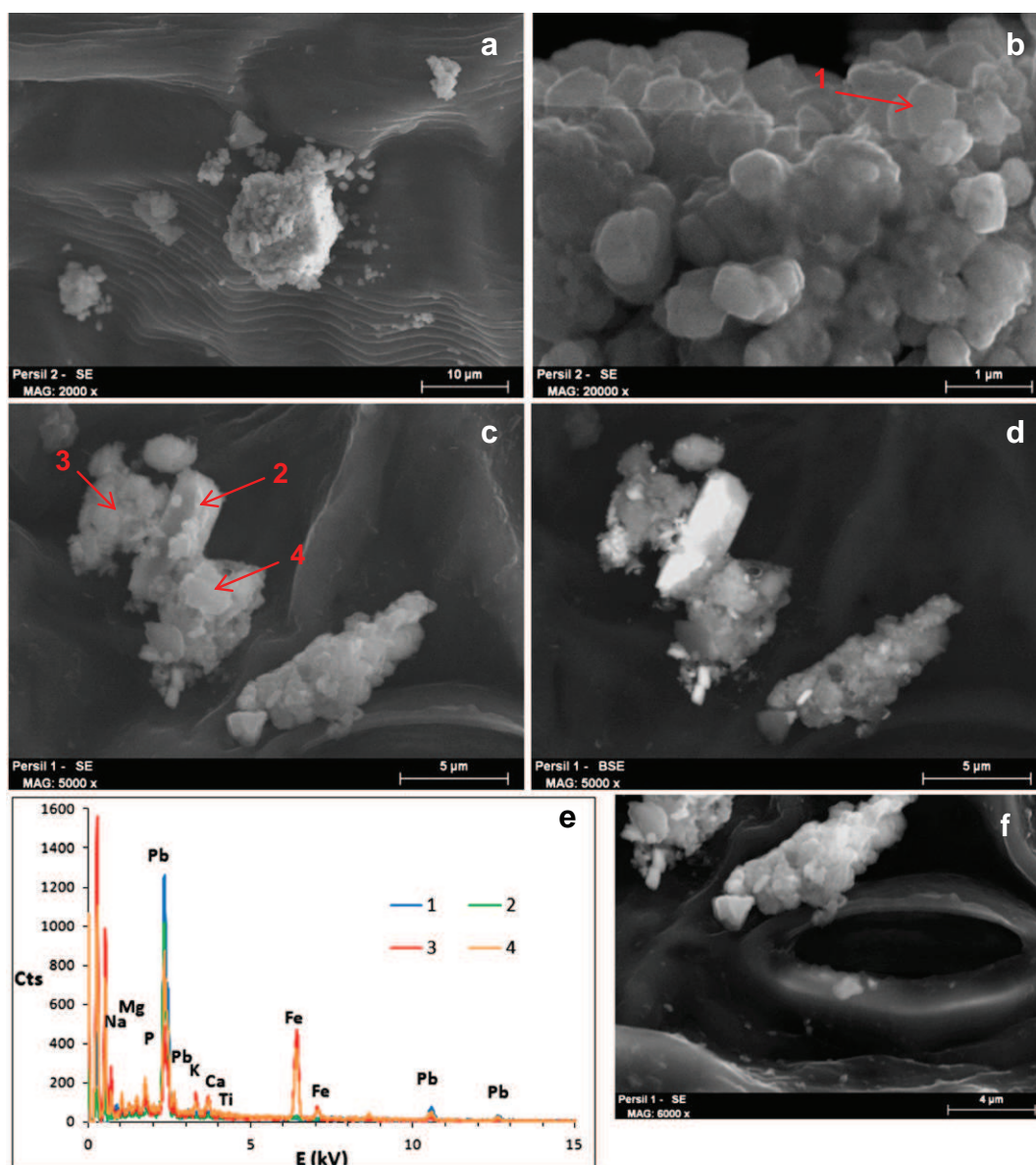
Fig. 4. SEM-EDX analyses of the surface of parsley leaf. Particles 1 and 2 correspond to metallic Pb. Particles 3 and 4 are enriched in Fe and also contain Pb, K and Ca. Some particles are observed near and at the edge of the stomata (f).

some lead-rich particles internalized within plant tissues (Fig. 5-b and -c).

3.2.1. Surface imaging and depth profiling of the lead-containing necrotic zone in lettuces

Metal-containing necrotic zones located at the surface of lettuce leaves were complementarily analyzed using ToF-SIMS. This technique was used previously to study the distribution of metals (Becker et al., 2008), nutrients (Metzner et al., 2008) and organic compounds (Jetter and Sodhi, 2011) in plant leaves, but it is the first use for localization of metal-rich PM and their secondary compounds.

A lot of observations and Tof-SIMS analyses were performed on necrosis and lead-enriched specific zones of the leaves. Only the most interesting and representative results are presented in this work. Positive and negative ion spectra obtained from the leaf surface and necroses-lead free were investigated (not shown) and compared those of the lead-rich zone. The molecular image of a Pb-rich necrosis in positive mode was reconstructed and is presented in Fig. S3. The peak of $C_2H_5^+$ at m/z 29 was defined as typical of the organic layer on the leaf surface (cuticle). The peak of Ca^+ at m/z 40 was typically found in

positive ion spectra of the necrotic zone, confirming the EDX analysis. Characteristic peaks of Pb isotopes [206]Pb, [207]Pb and [208]Pb were found on the central zone of the necrosis as observed on the elemental maps. The isotopic ratios of lead in the Pb-rich zones were 24% [206]Pb, 22% [207]Pb and 52%[208]Pb, allowing for correct assignment of all molecular fragments containing Pb. On the surface, the peak intensities of the Pb^+ molecular fragments were low. Thus, determining lead speciation at the leaf surface was not possible. Depth profiling of this area was performed using a Cs^+ sputtering beam. Molecular images in positive and negative modes were recorded after the profiling (not shown). The profile for characteristic positive molecular fragments (Fig. 6) clearly indicated a decrease in the $C_2H_5^+$ fragment, which is related to an organic layer, whereas the molecular fragments related to Pb increased. New Pb fragments such as $PbSO_2^+$, PbO^+ and $PbCO^+$ clearly appeared when the thin organic layer was removed, indicating the presence of Pb compounds beneath the organic layer (estimated to be about 5 nm thick). Identification of $PbSO_2^+$, PbO^+ and $PbCO^+$ fragments agreed with the Pb species previously identified in necrotic zones, including $PbSO_4$ and $PbCO_3$ (Uzu et al., 2010) and correspond to primary particles.
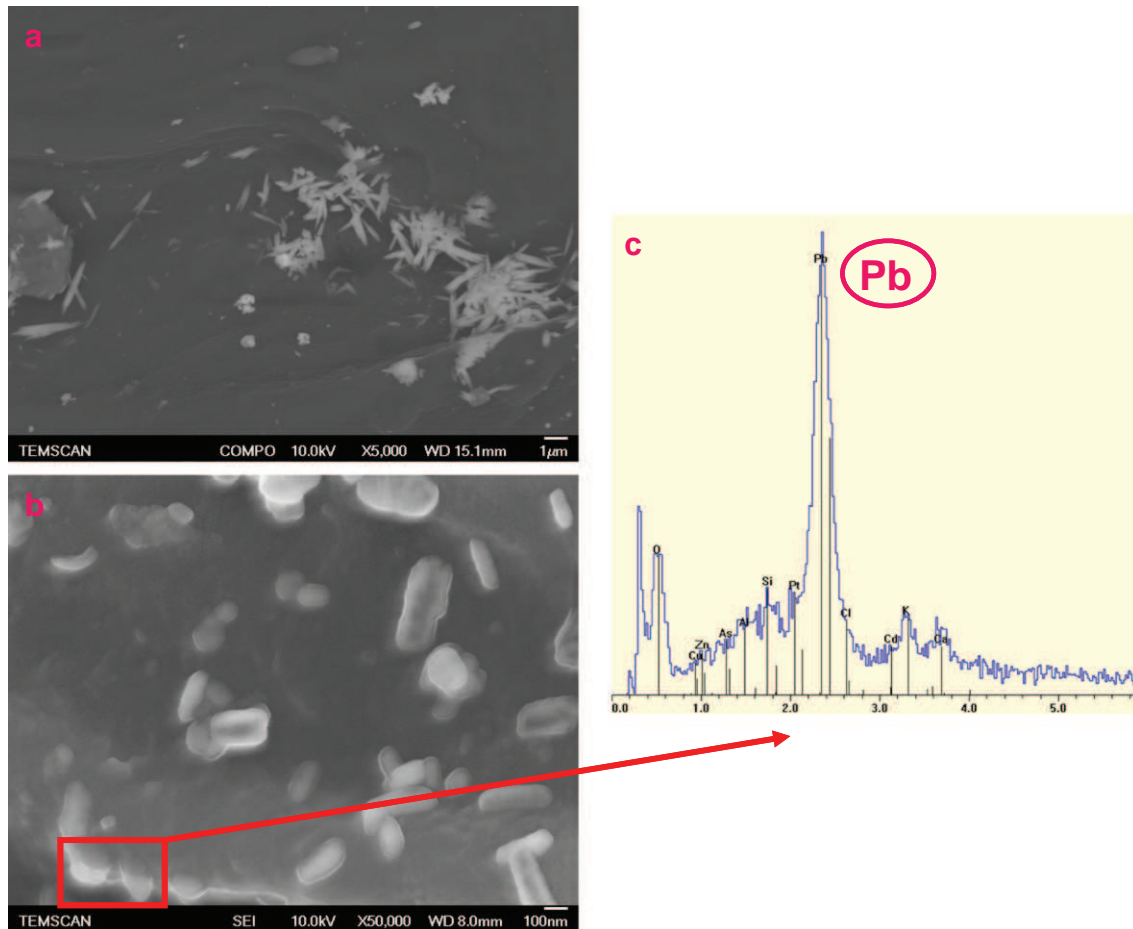
Fig. 5. SEM-EDX observations of Pb-containing secondary compounds observed on the leaf surface. a. Needle crystallites enriched in Pb were observed in the parsley surface. b. By zooming, some particles seemed to be currently in the way of a potential internalization. c. Spectrum showed that lead is the major component of internalized particles.

The Pb + fragments predominated in the upper part of the profile (between 20 and 1000 s sputtering time), with $PbSO_2^+$ as the major species at this depth. This result was confirmed by ToF-SIMS images recorded after depth profiling, which predominantly showed localized $PbSO_2^+$ (Fig. S3). The difference observed between the surface and depth analyses may be explained by differences in lead speciation at the surface compared to below the surface, but this hypothesis needs to be confirmed. ToF-SIMS observations clearly showed the

Fig. 6. Depth profiling of a lead-rich necrosis obtained by ToF-SIMS.

internalization in leaf cuticle tissues of lead-containing particles as primary PM without any biogeochemical transformation.

3.2.2. Proposed potential foliar pathways

As previously suggested by electron microscopy (Fig. 5), particles might be found on the surface of the leaves in a strongly agglomerated form. They might be trapped by the cuticular wax and then diffused in the leaf tissue (after dissolution or translocation through the cuticle). Honour et al. (2009) reported that leaf surface characteristics were affected by pollutant exposure: contact angle measurements indicated changes in surface wax structure, suggesting a role of this external protection mechanism in particle incorporation. The ToF-SIMS results were consistent with particle penetration through the cuticle, as suggested by the presence of Pb compounds beneath the organic layer. Ward (1990) reported that several metals such as Co, Cu or Mn could cross the cuticle. Grantz et al. (2003) suggested that PM deposition could involve vegetative surface injuries and the uptake of materials, such as metals, across the cuticle. According to Chamberlain (1983) and Nair et al. (2010), this phenomenon depends on cuticle maturity and environmental factors. The thickness of the organic layer above the internalized primary compounds (about 5 nm) indicates that the process could be a kind of internalization throughout the cuticle wax. Birbaum et al. (2010) reported that wax lipids may quickly adsorb on the large surface of the particles. This hypothesis was confirmed by Schreiber (2005), who reported polar paths of diffusion across plant cuticles, suggesting a new way for uptake of ionic compounds.

After diffusion through the cuticle, ultrafine particles may interact with cells. As reported by Birbaum et al. (2010) for cerium dioxide nanoparticles, fine particles can easily cross biological barriers such as
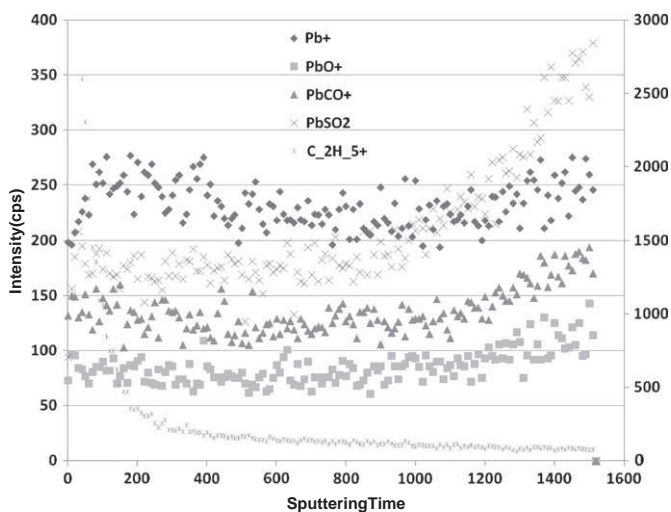
the cell wall of plants. Nair et al. (2010) reported that nanoparticles could be internalized during endocytosis with the help of a cavity-like structure formed by a plasma membrane. Moreover, working on lead absorption by root cells of maize, Raven et al. (1999) reported that endocytosis via integral membrane proteins (IMPs) occurred in specialized regions of the plasma membrane. Contrary to stomata pathways which are not selective, uptake through the cuticle could be strongly affected by physicochemical interactions between the solutes or particles and cuticular components (Schönherr and Schreiber, 2004). The membrane could invaginate and form a vesicle, allowing internalization of lead compounds in the root cell. Measurements using transmission electron microscopy on leaf sections should be acquired to test this hypothesis.

4. Conclusions

This study showed for the first time a multi-element foliar uptake and the accumulation of Pb, Cu, Zn, Cd, Sn, Sb and As for plants exposed to atmospheric PM fallouts emitted by a lead-battery recycling factory. Metal concentrations differed in the three plant species, with ryegrass being the highest metal accumulator. The different washing procedures used could not account for these differences, suggesting an influence of the plant species, possibly related to their morphology and physiology. The use of complementary techniques (μXRF, SEM-EDX and ToF-SIMS) allowed the investigation of leaves at different scales and provided information on chemical associations, morphology and speciation of lead compounds at different depths from the leaf surface. After deposition of metal-enriched particles, internalization through the cuticle and penetration through stomatal openings might represent major pathways for metal entry.

The internalization of Pb-rich particles and changes in metal speciation observed have (i) environmental implications since leaves affect the fate of Pb-rich particles after deposition, and (ii) health implications since crops represent an entry point for metals in the food chain (in the present case, for human and cattle), and metal speciation is closely related to their bioaccessibility.

Appendix A. Supplementary data

Supplementary data to this article can be found online at doi:10.1016/j.scitotenv.2012.03.051.

References

Alexander PD, Alloway BJ, Dourado AM. Genotypic variations in the accumulation of Cd, Cu, Pb and Zn exhibited by six commonly grown vegetables. Environ Pollut 2006;144:736–45.

Auffan M, Rose J, Bottero JY, Lowry GV, Jolivet JP, Wiesner MR. Towards a definition of inorganic nanoparticles from an environmental, health and safety perspective. Nat Nanotechnol 2009a;4:634–41.

Auffan M, Rose J, Wiesner M, Bottero JY. Chemical stability of metallic nanoparticles: A parameter controlling their potential cellular toxicity in vitro. Environ Pollut 2009b;157:1127–33.

Barber JL, Thomas GO, Kerstiens G, Jones KC. Current issues and uncertainties in the measurement and modelling of air–vegetation exchange and within-plant processing of POPs. Environ Pollut 2004;128:99-138.

Batonneau Y, Bremard C, Gengembre L, Laureyns J, Le Maguer A, Le Maguer D, et al. Speciation of PM10 sources of airborne nonferrous metals within the 3-km zone of lead/zinc smelters. Environ Sci Technol 2004;38:5281–9.

Becker JS, Dietrich RC, Matusch A, Pozebon D, Dressier VL. Quantitative images of metals in plant tissues measured by laser ablation inductively coupled plasma mass spectrometry. Spectrochim Acta Part B 2008;63:1248–52.

Bermudez GMA, Rodriguez JH, Pignata ML. Comparison of the air pollution biomonitoring ability of three Tillandsia species and the lichen Ramalina celastri in Argentina. Environ Res 2009;109:6-14.

Birbaum K, Brogiolo R, Schellenberg M, Martinoia E, Stark WJ, Günther D, et al. No evidence for cerium dioxide nanoparticle translocation in maize plants. Environ Sci Technol 2010;44:8718–23.

Caggiano R, D'Emilio M, Macchiato M, Ragosta M. Heavy metals in rye-grass species versus metal concentrations in atmospheric particulate measured in an industrial area of southern Italy. Environ Monit Assess 2005;102:67–84.

Catinon M, Ayrault S, Daudin L, Sevin L, Asta J, Tissut M, et al. Atmospheric inorganic contaminants and their distribution inside stem tissues of Fraxinus excelsior L. Atmos Environ 2008;42:1223–38.

Cecchi M, Dumat C, Alric A, Felix-Faure B, Pradere P, Guiresse M. Multi-metal contamination of a calcic cambisol by fallout from a lead-recycling plant. Geoderma 2008;144:287–98.

Chamberlain AC. Fallout of lead and uptake by crops. Atmos Environ 1983;17:693–706.

Chessel D, Dufour AB, Thioulouse J. The ade4 package − I: one-table methods. R News 2004;4:5-10.

Da Cunha KPV, Do Nascimento CWA. Silicon effects on metal tolerance and structural changes in maize (Zea mays L.) grown on a cadmium and zinc enriched soil. Water Air Soil Pollut 2009;197:323–30.

Dall'Osto M, Harrison RM, Highwood EJ, O'Dowd C, Ceburnis D, Querol X, et al. Variation of the mixing state of Saharan dust particles with atmospheric transport. Atmos Environ 2010;44:3135–46.

Donisa C, Mocanu R, Steinnes E, Vasu A. Heavy metal pollution by atmospheric transport in natural soils from the northern part of eastern Carpathians. Water Air Soil Pollut 2000;120:347–58.

Eichert T, Goldbach HE. Equivalent pore radii of hydrophilic foliar uptake routes in stomatous and astomatous leaf surfaces − further evidence for a stomatal pathway. Physiol Plant 2008;132:491–502.

Eichert T, Kurt A, Steiner U, Goldbach HE. Size exclusion limits and lateral heterogeneity of the stomatal foliar uptake pathway for aqueous solutes and water-suspended nanoparticles. Physiol Plant 2008;134:151–60.

Ettler V, Johan Z, Baronnet A, Jankovský F, Gilles C, Mihaljevi M, et al. Mineralogy of air-pollution-control residues from a secondary lead smelter: environmental implications. Environ Sci Technol 2005;39:9309–16.

European Commission. Commission Regulation (EC) No 221/2002 of 6 February 2002 amending regulation (EC) no. 466/2001setting maximum levels for certain contaminants in foodstuffs. Official Journal of the European Communities; 2002.

Fernández Espinosa AJ, Ternero Rodríguez M, Barragán de la Rosa FJ, Jiménez Sánchez JC. A chemical speciation of trace metals for fine urban particles. Atmos Environ 2002;36:773–80.

Fernandez V, Eichert T. Uptake of hydrophilic solutes through plant leaves: current state of knowledge and perspectives of foliar fertilization. Crit Rev Plant Sci 2009;28:36–68.

Gandois L, Tipping E, Dumat C, Probst A. Canopy influence on trace metal atmospheric inputs on forest ecosystems: speciation in throughfall. Atmos Environ 2010;44:824–33.

Garrec JP, Van Haluwyn C. Biosurveillance végétale de la qualité de l'air. Concepts, méthodes et applications. Tec et Doc; 2002. Editions, 118 pp.

Godinho RM, Wolterbeek HT, Pinheiro MT, Alves LC, Verburg TG, Freitas MC. Microscale elemental distribution in the thallus of Flavoparmelia caperata transplanted to polluted site. J Radioanal Nucl Chem 2009;281:205-2010.

Gonzalez-Miqueo L, Elustondo D, Lasheras E, Santamaria JM. Use of native mosses as biomonitors of heavy metals and nitrogen deposition in the surroundings of two steel works. Chemosphere 2010;78:965–71.

Grantz DA, Garner JHB, Johnson DW. Ecological effects of particulate matter. Environ Int 2003;29:213–39.

Grzegorzewski F, Rohn S, Kroh LW, Geyer M, Schlüter O. Surface morphology and chemical composition of lamb's lettuce (Valerianella locusta) after exposure to a low-pressure oxygen plasma. Food Chem 2010;122:1145–52.

Guderian R, Tingey DT, Rake R. Effects of photochemical oxidants on plants. In: Guderian R, editor. Air pollution by photochemical oxidants. New York, USA: Springer-Verlag; 1985.

Honour SL, Bell JNB, Ashenden TWA, Cape JN, Power SA. Responses of herbaceous plants to urban air pollution: effects on growth, phenology and leaf surface characteristics. Environ Pollut 2009;157:1279–86.

Hu X, Zhang Y, Luo J, Xie M, Wang T, Lian H. Accumulation and quantitative estimates of airborne lead for a wild plant (Aster subulatus). Chemosphere 2011;82:1351–7.

Jetter R, Sodhi R. Chemical composition and microstructure of waxy plant surfaces: triterpenoids and fatty acid derivatives on leaves of Kalanchoe daigremontiana. Surf Interface Anal 2011;43:326–30.

Kabelitz L, Sievers H. Contaminants of medicinal and food herbs with a view of EU regulations. Inn Food Technol 2004;1:25–7.

Kozlov MV, Haukioja E, Bakhtiarov AV, Stroganov DN, Zimina SN. Root versus canopy uptake of heavy metals by birch in an industrially polluted area: contrasting behaviour of nickel and copper. Environ Pollut 2000;107:413–20.

Lee W, An Y, Yoon H. Toxicity and bioavailability of copper nanoparticles to the terrestrials plants mung bean (Phaseolus radiatus) and wheat (Triticum awstivum): plant uptake for water insoluble nanoparticles. Environ Toxicol Chem 2008;27:1915–21.

Lin D, Xing B. Phytotoxicity of nanoparticles: Inhibition of seed germination and root growth. Environ Pollut 2007;150:243–50.

Lin D, Xing B. Root uptake and phytotoxicity of ZnO nanoparticles. Environ Sci Technol 2008;42:5580–5.

Lindow SE, Brandl MT. Microbiology of the phyllosphere. Appl Environ Microbiol 2003;69:1875–83.

Little PE. Deposition of exhaust lead and its impact on plants. Symposium "The impact of road traffic on plants" — September 1978, 513. TRRL, supplementary report; 1978. p. 49–54.

Lombi E, Scheckel KG, Kempsond IM. In situ analysis of metal(loid)s in plants: state of the art and artefacts. Environ Exp Bot 2011;72:3-17.

Ma X, Geiser-Lee J, Deng Y, Kolmakov A. Interactions between engineered nanoparticles (ENPs) and plants: phytotoxicity, uptake and accumulation. Sci Total Environ 2010;16:3053–61.

Madany IM, Ali SM, Akhter MS. Assessment of lead in roadside vegetation in Bahrain. Environ Int 1990;16:123–6.

Metzner R, Schneider HU, Breuer U, Schroeder WH. Imaging nutrient distributions in plant tissue using time-of-flight secondary ion mass spectrometry and scanning electron microscopy. Plant Physiol 2008;147:1774–87.

Millhollen A, Gustin M, Obrist D. Foliar mercury accumulation and exchange for three tree species. Environ Sci Technol 2006;40:6001–6.

Moeckel C, Thomas G, Barber J, Jones K. Uptake and storage of PCBs by plant cuticles. Environ Sci Technol 2008;42:100–5.

Munksgaard NC, Parry UDL. Lead isotope ratios determined by ICP-MS: monitoring of mining-derived metal particulates in atmospheric fallout, Northern Territory, Australia. Sci Total Environ 1998;217:113–25.

Nair R, Varghese S, Nair B, Maekawa T, Yoshida Y, Kumar D. Nanoparticulate material delivery to plants. Plant Sci 2010;179:154–63.

NF X43-901. Biosurveillance de l'air - Biosurveillance active de la qualité de l'air à l'aide de ray-grass : des cultures à la préparation des échantillons. AFNOR – Association Française de Normalisation, La Plaine Saint-Denis (FRA); 2008.

Pascault N, Cécillon L, Mathieu O, Hénault C, Sarr A, Lévêque J, et al. In situ dynamics of microbial communities during decomposition of wheat, rape and alfalfa residues. Microb Ecol 2010;60:816–28.

Perkins MC, Roberts CJ, Briggs D, Davies MC, Friedmann A, Hart CA, et al. Surface morphology and chemistry of Prunus laurocerasus L. leaves: a study using X-ray photoelectron spectroscopy, time-of-flight secondary-ion mass spectrometry, atomic-force microscopy and scanning-electron microscopy. Planta 2005;221:123–34.

Perrone MG, Gualtieri M, Ferrero L, Lo Porto C, Udisti R, Bolzacchini E, et al. Seasonal variations in chemical composition and in vitro biological effects of fine PM from Milan. Chemosphere 2010;78:1368–77.

Polichetti G, Cocco S, Spinali A, Trimarco V, Nunziata A. Effects of particulate matter (PM_{10}, $PM_{2.5}$ and PM_1) on the cardiovascular system. Toxicology 2009;261:1–8.

R Development Core Team. R: a language and environment for statistical computing. Vienna, Austria: R Foundation for Statistical Computing3-900051-07-0; 2010. URL http://www.R-project.org/.

Rao MV, Dubey PS. Occurrence of heavy metals in air and their accumulation by tropical plants growing around an industrial area. Sci Total Environ 1992;126:1-16.

Raven PH, Evert RF, Eichhorn SE. Biology of plants. 6th ed. New York: W. H. Freeman and Company; 1999.

Richmond KE, Sussman M. Got silicon? The non-essential beneficial plant nutrient. Curr Opin Plant Biol 2003;6:268–72.

Rodriguez JA, Nanos N, Grau JM, Gil L, Lopez-Arias M. Multiscale analysis of heavy metal contents in Spanish agricultural topsoils. Chemosphere 2008;70:1085–96.

Rossini Oliva S, Mingorance MD. Assessment of airborne heavy metal pollution by aboveground plant parts. Chemosphere 2006;65:177–82.

Schönherr J. Characterization of aqueous pores in plant cuticles and permeation of ionic solutes. J Exp Bot 2006;57:2471–91.

Schönherr J, Luber M. Cuticular penetration of potassium salts: effects of humidity, anions and temperature. Plant Soil 2001;236:117–22.

Schönherr J, Schreiber L. Size selectivity of aqueous pores in astomatous cuticular membranes isolated from Populus canescens (Aiton) Sm. leaves. Planta 2004;219: 405–11.

Schreck E, Foucault Y, Geret F, Pradere P, Dumat C. Influence of soil ageing on bioavailability and ecotoxicity of lead carried by process waste metallic ultrafine particles. Chemosphere 2011;85:1555:1562-1555:.

Schreiber L. Polar paths of diffusion across plant cuticles: new evidence for an old hypothesis. Ann Bot 2005;95:1069–73.

Schreiber L, Schönherr J. Phase transitions and thermal expansion coefficients of plant cuticles: the effect of temperature on structure and function. Planta 1992;182:186–93.

Spagnuolo V, Zampella M, Giordano S, Adamo P. Cytological stress and element uptake in moss and lichen exposed in bags in urban area. Ecotoxicol Environ Saf 2011;74: 1434–43.

Stamenkovic J, Gustin M. Nonstomatal versus stomatal uptake of atmospheric mercury. Environ Sci Technol 2009;43:1367–72.

Stampoulis D, Sinha SK, White JC. Assay-dependent phytotoxicity of nanoparticles to plants. Environ Sci Technol 2009;43:9473–9.

Tomasevic M, Vukmirovic Z, Rajsic S, Tasic M, Stevanovic B. Characterization of trace metal particles deposited on some deciduous tree leaves in an urban area. Chemosphere 2005;61:753–60.

Uzu G, Sobanska S, Aliouane Y, Pradere P, Dumat C. Study of lead phytoavailability for atmospheric industrial micronic and sub-micronic particles in relation with lead speciation. Environ Pollut 2009;157:1178–85.

Uzu G, Sobanska S, Sarret G, Munoz M, Dumat C. Foliar lead uptake by lettuce exposed to atmospheric fallouts. Environ Sci Technol 2010;44:1036–42.

Uzu G, Sobanska S, Sarret G, Sauvain JJ, Pradère P, Dumat C. Characterization of lead-recycling facility emissions at various workplaces: major insights for sanitary risk assessment. J Hazard Mater 2011a;186:1018–27.

Uzu G, Sauvain JJ, Baeza-Squiban A, Riediker M, Sánchez Sandoval HM, Val S, et al. In vitro assessment of the pulmonary toxicity and gastric availability of lead-rich particles from a recycling plant. Environ Sci Technol 2011b;45:7888–95.

Waisberg M, Black WD, Waisberg CM, Hale B. The effect of pH, time and dietary source of cadmium on the bioaccessibility and adsorption of cadmium to/from lettuce (Lactuca sativa L. cv. Ostinata). Food Chem Toxicol 2004;42:835–42.

Ward NI. Lead contamination of the London orbital (M25) motorway (since it's opening in 1986). Sci Total Environ 1990;93:277–84.

Ward NI, Savage JM. Metal dispersion and transportational activities using foog crops as biomonitors. Sci Total Environ 1994;146–147:309–19.

WHO. Air quality guidelines for Europe European series; 1987. number 23.

Yin L, Cheng Y, Espinasse B, Colman BP, Auffan M, Wiesner M, et al. More than the ions: the effects of silver nanoparticles on Lolium multiflorum. Environ Sci Technol 2011;45: 2360–7.